

Thermodynamics of Kerr-Newman-AdS Black Holes and Conformal Field Theories

Marco M. Caldarelli*, Guido Cognola† and Dietmar Klemm‡

*Università degli Studi di Trento,
Dipartimento di Fisica,
Via Sommarive 14
38050 Povo (TN)
Italia*

*and
Istituto Nazionale di Fisica Nucleare,
Gruppo Collegato di Trento,
Italia*

Abstract

We study the thermodynamics of four-dimensional Kerr-Newman-AdS black holes both in the canonical and the grand-canonical ensemble. The stability conditions are investigated, and the complete phase diagrams are obtained, which include the Hawking-Page phase transition in the grand-canonical ensemble. In the canonical case, one has a first order transition between small and large black holes, which disappears for sufficiently large electric charge or angular momentum. This disappearance corresponds to a critical point in the phase diagram. Via the AdS/CFT conjecture, the obtained phase structure is also relevant for the corresponding conformal field theory living in a rotating Einstein universe, in the presence of a global background $U(1)$ current. An interesting limit arises when the black holes preserve some supersymmetry. These BPS black holes correspond to highly degenerate zero temperature states in the dual CFT, which lives in an Einstein universe rotating with the

*email: caldarel@science.unitn.it

†email: cognola@science.unitn.it

‡email: klemm@science.unitn.it

speed of light.

04.70.-s, 11.25.Hf, 04.60.-m, 04.65.+e

I. INTRODUCTION

The conjectured equivalence of string theory on anti-de Sitter (AdS) spaces (times some compact manifold) and certain superconformal gauge theories living on the boundary of AdS [1–4] has lead to an increasing interest in asymptotically anti-de Sitter black holes. This interest is mainly based on the fact that the classical supergravity black hole solution can furnish important informations on the dual gauge theory in the large N limit, N denoting the rank of the gauge group. The standard example of this is the well-known Schwarzschild-AdS black hole, whose thermodynamics was studied 17 years ago by Hawking and Page [5], who discovered a phase transition from thermal AdS space to a black hole phase, as the temperature increases. This means that at a certain temperature thermal radiation in AdS space becomes unstable, and eventually collapses to form a black hole. The Hawking-Page phase transition was then reconsidered by Witten [6] in the spirit of the AdS/CFT correspondence. He observed that it can be interpreted as a transition from a low-temperature confining to a high temperature deconfining phase in the dual field theory.

Up to now, the study of black holes in the context of the AdS/CFT correspondence has been extended in various directions, e. g. to black holes with non-spherical event horizon topologies [7–9] or to electrically charged Reissner-Nordström-AdS (RNAdS) solutions [10,11], following previous work on this subject performed in [12–15]. Thereby, some interesting observations have been made, like the striking resemblance of the RNAdS phase structure to that of the van der Waals-Maxwell liquid-gas system [10,11]¹, or the possible appearance of so-called “precursor” states [16] in the CFT dual of hyperbolic black holes [9]. Furthermore, the thermodynamics of R-charged black holes in four, five and seven dimensions has been studied in detail in [17]. Another interesting extension is the inclusion of rotation, i. e. the consideration of Kerr-AdS black holes [18,19]². In this case, the dual CFT lives in a rotating Einstein universe [18]. The authors of [18] studied the limit of critical angular velocity, at which this Einstein universe rotates with the speed of light, from both the CFT and the bulk side. Recently, the AdS/CFT correspondence has been probed in [21] by comparing in more detail the thermodynamics of rotating black holes in five-dimensional anti-de Sitter space with that of $\mathcal{N} = 4$ super Yang-Mills theory on a rotating Einstein universe in four dimensions.

In the present paper, we shall consider the charged rotating case, i. e. Kerr-Newman-AdS (KNAdS) solutions. (Note that the appearance of second-order phase transitions for Kerr-Newman black holes in de Sitter space, i. e. for positive cosmological constant, was first shown by Davies [22]).

The remainder of this article is organized as follows:

In section II we review the four-dimensional KNAdS black hole, give the conserved quantities like mass and angular momentum, and recall the conditions under which some amount

¹A similar phase structure has recently been found by considering stringy corrections to AdS black holes [8].

²For a discussion of Kerr-NUT-AdS and Kerr-bolt-AdS spacetimes cf. [20].

of supersymmetry is preserved. In III we calculate the Euclidean action, using the method of counterterms introduced in [23–26]. In section IV the black hole thermodynamics is considered in both the canonical and grand canonical ensemble. The resulting phase structure is elaborated, and the thermodynamical stability of the solutions is studied. Finally, in V our results are summarized and discussed in the context of the conformal field theory in the rotating Einstein universe.

II. KERR-NEWMAN-ADS BLACK HOLES

Here we consider the usual charged rotating black hole in AdS space. Its horizon is homeomorphic to a sphere, and its metric, which is axisymmetric, reads in Boyer-Lindquist-type coordinates [27,28]

$$ds^2 = -\frac{\Delta_r}{\rho^2} \left[dt - \frac{a \sin^2 \theta}{\Xi} d\phi \right]^2 + \frac{\rho^2}{\Delta_r} dr^2 + \frac{\rho^2}{\Delta_\theta} d\theta^2 + \frac{\Delta_\theta \sin^2 \theta}{\rho^2} \left[a dt - \frac{r^2 + a^2}{\Xi} d\phi \right]^2, \quad (1)$$

where

$$\rho^2 = r^2 + a^2 \cos^2 \theta, \quad \Xi = 1 - \frac{a^2}{l^2}, \quad (2)$$

$$\Delta_r = (r^2 + a^2) \left(1 + \frac{r^2}{l^2} \right) - 2mr + z^2, \quad \Delta_\theta = 1 - \frac{a^2}{l^2} \cos^2 \theta. \quad (3)$$

Here a denotes the rotational parameter and z is defined by $z^2 = q_e^2 + q_m^2$, q_e and q_m being electric and magnetic charge parameters respectively.

The metric (1) solves the Einstein-Maxwell field equations with an electromagnetic vector potential and an associated field strength tensor respectively given by

$$A = -\frac{q_e r}{\rho \sqrt{\Delta_r}} e^0 - \frac{q_m \cos \theta}{\rho \sqrt{\Delta_\theta} \sin \theta} e^3, \quad (4)$$

and

$$F = -\frac{1}{\rho^4} [q_e(r^2 - a^2 \cos^2 \theta) + 2q_m r a \cos \theta] e^0 \wedge e^1 + \frac{1}{\rho^4} [q_m(r^2 - a^2 \cos^2 \theta) - 2q_e r a \cos \theta] e^2 \wedge e^3, \quad (5)$$

where we have defined the vierbein field

$$e^0 = \frac{\sqrt{\Delta_r}}{\rho} (dt - \frac{a \sin^2 \theta}{\Xi} d\phi), \quad e^1 = \frac{\rho}{\sqrt{\Delta_r}} dr, \quad (6)$$

$$e^2 = \frac{\rho}{\sqrt{\Delta_\theta}} d\theta, \quad e^3 = \frac{\sqrt{\Delta_\theta} \sin \theta}{\rho} (a dt - \frac{r^2 + a^2}{\Xi} d\phi). \quad (7)$$

Let us define the critical mass parameter m_{extr} ,

$$m_{extr}(a, z) = \frac{l}{3\sqrt{6}} \left(\sqrt{\left(1 + \frac{a^2}{l^2}\right)^2 + \frac{12}{l^2}(a^2 + z^2) + \frac{2a^2}{l^2} + 2} \right) \\ \times \left(\sqrt{\left(1 + \frac{a^2}{l^2}\right)^2 + \frac{12}{l^2}(a^2 + z^2) - \frac{a^2}{l^2} - 1} \right)^{\frac{1}{2}}. \quad (8)$$

A study of the positive zeroes of the function Δ_r shows that the line element (1) describes a naked singularity for $m < m_{extr}$ ³ and a black hole with an outer event horizon and an inner Cauchy horizon for $m > m_{extr}$. Finally, for $m = m_{extr}$, the lapse function has a double root and (1) represents an extremal black hole. One should also note that the solution is valid only for $a^2 < l^2$; it becomes singular in the limit $a^2 = l^2$. In this critical limit, which has been studied extensively in Ref. [18] (cf. also [21]), the three dimensional Einstein universe at infinity rotates with the speed of light. Here we assume m to be larger than m_{extr} and $a < l$, so the metric (1) represents an AdS black hole, with an event horizon at $r = r_+$, where r_+ is the largest solution of $\Delta_r = 0$. For the horizon area one gets

$$\mathcal{A} = \frac{4\pi(r_+^2 + a^2)}{\Xi}. \quad (9)$$

Analytical continuation of the Lorentzian metric by $t \rightarrow i\tau$ and $a \rightarrow ia$ yields the Euclidean section, whose regularity at $r = r_+$ requires that we must identify $\tau \sim \tau + \beta$ and $\phi \sim \phi + i\beta\Omega_H$, where the inverse Hawking temperature β is given by

$$\beta = \frac{4\pi(r_+^2 + a^2)}{r_+ \left(1 + \frac{a^2}{l^2} + 3\frac{r_+^2}{l^2} - \frac{a^2 + z^2}{r_+^2} \right)}, \quad (10)$$

and

$$\Omega_H = \frac{a\Xi}{r_+^2 + a^2} \quad (11)$$

represents the angular velocity of the event horizon. Ω_H can also be obtained by using the fact that the surface $r = r_+$ is a bolt of the co-rotating Killing vector $\partial_\tau + i\Omega_H\partial_\phi$ in the Euclidean section. One can also write the metric (1) in the canonical form

$$ds^2 = -N^2 dt^2 + \frac{\rho^2}{\Delta_r} dr^2 + \frac{\rho^2}{\Delta_\theta} d\theta^2 + \frac{\Sigma^2 \sin^2 \theta}{\rho^2 \Xi^2} (d\phi - \omega dt)^2, \quad (12)$$

where

$$\Sigma^2 = (r^2 + a^2)^2 \Delta_\theta - a^2 \Delta_r \sin^2 \theta, \quad (13)$$

³Note that the solution with $m = z = 0$ describes AdS space seen by a rotating observer.

and the lapse function N and the angular velocity ω are defined by

$$N^2 = \frac{\rho^2 \Delta_r \Delta_\theta}{\Sigma^2}, \quad (14)$$

$$\omega = \frac{a\Xi}{\Sigma^2} [\Delta_\theta(r^2 + a^2) - \Delta_r] \quad (15)$$

respectively. Note that $\omega = \Omega_H$ on the horizon, whereas $\omega = -a/l^2 \equiv \Omega_\infty$ for $r \rightarrow \infty$. The fact that the angular velocity does not vanish at infinity is a salient feature of rotating black holes in AdS space, different from the asymptotically flat case, where $\Omega_\infty = 0$. The angular velocity Ω entering the thermodynamics is then given by the *difference*

$$\Omega = \Omega_H - \Omega_\infty, \quad (16)$$

analogously to the case of an electric potential. For asymptotically flat spacetimes, (16) reduces to $\Omega = \Omega_H$, but for the KNAdS black hole we get

$$\Omega = \Omega_H + \frac{a}{l^2} = \frac{a(1 + r_+^2/l^2)}{r_+^2 + a^2}. \quad (17)$$

This is exactly the angular velocity of the rotating Einstein universe at infinity [18]. To see this, one first applies an implicit coordinate transformation, which takes the standard AdS metric to the $m = z = 0$ KNAdS form [18]. (17) can then be read off from the transformation rule of the coordinate ϕ .

The fact that the angular velocity relevant to Kerr-Newman-AdS black hole thermodynamics turns out to be the one of the rotating Einstein universe at the AdS boundary, agrees nicely with the AdS/CFT correspondence: If the KNAdS black hole in the bulk is described by a conformal field theory living on the boundary, then the relevant angular velocity entering the thermodynamics should be that of the rotating Einstein universe at infinity.

Moreover, when $\Omega < 1/l$, a timelike killing vector can be globally defined outside the event horizon [18], in contrast to the asymptotically flat case. Then the rotating black hole can be in equilibrium with rotating thermal radiation all the way out to infinity, and a consistent thermodynamics can be defined. When this condition is fulfilled, the rotating Einstein universe spins slower than light, and an associated state can be defined on the boundary CFT. This is closely related with the fact that for $\Omega < 1/l$ there are no superradiant modes [19].

The mass M and the angular momentum J can be defined by means of Komar integrals, using the Killing vectors ∂_t/Ξ and ∂_ϕ ⁴. Taking AdS space as reference background, one gets

$$M = \frac{m}{\Xi^2}, \quad J = \frac{am}{\Xi^2}. \quad (18)$$

The charges are obtained by computing the flux of the electromagnetic field tensor at infinity, yielding

⁴We have normalized the Killing vectors so that the corresponding conserved quantities generate the algebra $so(3,2)$, like it was done in Ref. [29].

$$Q_e = \frac{q_e}{\Xi}, \quad Q_m = \frac{q_m}{\Xi}. \quad (19)$$

The electric potential Φ , measured at infinity with respect to the horizon, is defined by

$$\Phi = A_a^e \chi^a|_{r \rightarrow \infty} - A_a^e \chi^a|_{r=r_+} = \frac{q_e r_+}{r_+^2 + a^2}, \quad (20)$$

where $\chi = \partial_t + \Omega_H \partial_\phi$ is the null generator of the horizon and A_a^e denotes the electric part of the vector potential.

Finally, let us recall the conditions under which some amount of supersymmetry is preserved by the Kerr-Newman-AdS black holes. These objects were considered in [29,30] in the context of gauged $N = 2$, $D = 4$ supergravity. There it was found that for

$$m^2 = la \left(1 + \frac{a}{l}\right)^4, \quad q_e^2 = la \left(1 + \frac{a}{l}\right)^2, \quad q_m = 0 \quad (21)$$

the KNAdS black holes preserve half of the supersymmetries. In the BPS limit we have

$$M = \frac{\sqrt{la}}{\left(1 - \frac{a}{l}\right)^2}, \quad Q_e = \frac{\sqrt{la}}{1 - \frac{a}{l}}, \quad Q_m = 0, \quad J = \frac{\sqrt{la}a}{\left(1 - \frac{a}{l}\right)^2}, \quad (22)$$

so the Bogomol'nyi bound is [29]

$$M = Q_e + \frac{J}{l}. \quad (23)$$

Furthermore, in the supersymmetric case, one has the relations

$$r_+^2 = al, \quad \Omega = \frac{1}{l}. \quad (24)$$

The latter relation means that in the BPS limit, the Einstein universe at infinity, in which the dual conformal field theory lives, rotates effectively with the speed of light. An analogous situation was found in Ref. [18] for the supersymmetric rotating BTZ black hole.

III. EUCLIDEAN ACTION

We turn now to the calculation of the Euclidean action, which will then yield the thermodynamic potentials relevant to the various ensembles [31]. In the action computation one usually encounters infrared divergences, which are regularized by subtracting a suitably chosen background. Such a procedure, however, in general is not unique; in some cases the choice of reference background is ambiguous, e. g. for hyperbolic AdS black holes [32,24]. Recently, in order to regularize divergent integrals like those appearing in the computation of the Euclidean action, a different procedure has been proposed [23–26]. This technique was inspired by the AdS/CFT correspondence, and consists in adding suitable counterterms I_{ct} to the action. These counterterms are built up with curvature invariants of a boundary $\partial\mathcal{M}$ (which is sent to infinity after the integration), and thus obviously do not alter the bulk equations of motion. This kind of procedure, which will also be employed in the present

paper, has the advantage to be free of ambiguities, which, on the contrary, are present in the traditional approach in some particular cases, like mentioned above.

To start with, we write the Euclidean Einstein-Maxwell action in the form

$$I = I_{bulk} + I_{surf} + I_{ct} = -\frac{1}{16\pi G} \int_{\mathcal{M}} d^4x \sqrt{g} [R - 2\Lambda - F^2] - \frac{1}{8\pi G} \int_{\partial\mathcal{M}} d^3x \sqrt{h} K + I_{ct}, \quad (25)$$

$\Lambda = -3/l^2$ being the 4-dimensional cosmological constant, with l the radius of AdS space. The action (25) differs from the familiar one by the presence of the last term, which contains all surface counterterms needed to assure convergence of the integrals. In four dimensions it reads [24]

$$I_{ct} = \int_{\partial\mathcal{M}} d^3x \sqrt{h} \left[\frac{2}{l} + \frac{l}{2} \mathcal{R} - \frac{l^3}{2} \left(\mathcal{R}_{ab} \mathcal{R}^{ab} - \frac{3}{8} \mathcal{R}^2 \right) \right], \quad (26)$$

h_{ab} and \mathcal{R}_{ab} denoting the metric and Ricci curvature of the (arbitrary) boundary $\partial\mathcal{M}$.

The variation of the bulk integral with respect to the fields gives

$$\delta I = -\frac{1}{16\pi G} \int_{\mathcal{M}} d^4x \sqrt{g} \left[G_{ab} + \Lambda g_{ab} - \left(2F_a{}^c F_{bc} - \frac{1}{2} F^2 g_{ab} \right) \right] \delta g^{ab} - \frac{1}{4\pi G} \int_{\mathcal{M}} d^4x \sqrt{g} (\nabla_a F^{ab}) \delta A_b + \frac{1}{4\pi G} \int_{\partial\mathcal{M}} d^3x \sqrt{h} n_a F^{ab} \delta A_b, \quad (27)$$

where n^a is the outward pointing unit normal to $\partial\mathcal{M}$. Asking for a stationary point of the action, the bulk integrals in Eq. (27) yield the Einstein-Maxwell field equations

$$G_{ab} + \Lambda g_{ab} = T_{ab}, \quad \nabla_a F^{ab} = 0, \quad (28)$$

where we have defined the electromagnetic stress tensor

$$T_{ab} = 2F_a{}^c F_{cb} - \frac{1}{2} F^2 g_{ab}, \quad (29)$$

while the surface integral has to vanish to have a differentiable action functional and a well defined action principle. This imposes the boundary condition $\delta A_a = 0$ on $\partial\mathcal{M}$. This action is thus appropriate to study the ensemble with fixed electric potential Φ_e and fixed magnetic charge Q_m .

To study the canonical ensemble with fixed magnetic *and* electric charge, we have to add another boundary term to impose fixed Q_e as a boundary condition at infinity [33], restoring the electromagnetic duality. The appropriate action in this case is

$$\tilde{I} = I - \frac{1}{4\pi G} \int_{\partial\mathcal{M}} d^3x \sqrt{h} n_a F^{ab} A_b, \quad (30)$$

and its variation reads

$$\delta \tilde{I} = (\text{bulk terms}) - \frac{1}{4\pi G} \int_{\partial\mathcal{M}} d^3x \sqrt{h} A^b \delta (n^a F_{ab}). \quad (31)$$

The bulk contribution yields again the Einstein-Maxwell equations, while the vanishing of the surface term, needed to have a differentiable action functional, requires $\delta(n^a F_{ab}) = 0$ at infinity as a boundary condition.

Now the evaluation of the Euclidean action is a straightforward computation. First of all, on shell the bulk contribution simplifies to

$$I_{bulk} = \frac{1}{16\pi G} \int d^4x \sqrt{g} \left[F^2 + \frac{6}{l^2} \right]. \quad (32)$$

Then one chooses the boundary $\partial\mathcal{M} = S^1 \times S^2$, S^2 being a 2-sphere with a large radius, which has to be sent to infinity after the integration. Since the metric is stationary, the time integration gives rise to a simple multiplicative factor β . The integration on the other variables requires a little bit of work, but anyway it can be performed in a closed manner. The final results assume the form

$$I = \frac{\beta}{4Gl^2\Xi} \left[-r_+^3 + \Xi l^2 r_+ + \frac{l^2 a^2}{r_+} + \frac{l^2 (q_e^2 + q_m^2)}{r_+} - 2 \frac{l^2 (q_e^2 - q_m^2) r_+}{r_+^2 + a^2} \right], \quad (33)$$

$$\tilde{I} = \frac{\beta}{4Gl^2\Xi} \left[-r_+^3 + \Xi l^2 r_+ + \frac{l^2 (a^2 + z^2)}{r_+} + 2 \frac{l^2 z^2 r_+}{r_+^2 + a^2} \right], \quad (34)$$

valid for fixed potential and fixed charge respectively. In the following, we will consider only the case of vanishing magnetic charge, $q_m = 0$, so we set $q_e = q$ and $Q_e = Q$.

The behaviour of the obtained actions as functions of r_+ determines the thermodynamical properties of the black holes. It will be discussed in detail in section IV. Note that both actions are singular in the extremal case ($m = m_{extr}$) and also for $\Xi = 0$. The singularity for extremal black holes comes from the divergence of the inverse temperature β . Since one divides the action by β in order to obtain the thermodynamical potentials, the latter are well-defined also for $T = 0$.

In the last section we have already indicated how to calculate physical conserved quantities by evaluating Komar integrals. This traditional technique involves the subtraction of a suitably chosen reference background (in our case AdS space), in order to regularize infrared-divergent integrals. In the approach we are considering, instead, one does not use any reference background, and so it seems quite natural to compute the conserved charges by the direct use of the finite action (25), applying the method developed by Brown and York [34].

Let us briefly describe how this formalism works. We indicate by u^a the unit normal vector of a spacelike hyper-surface ${}^3\mathcal{S}_t$ at constant t and by $\partial\mathcal{M}$ the spatial boundary of the spacetime manifold \mathcal{M} , with induced metric h_{ab} . Moreover, $\Sigma = S^2$ is the spacelike intersection ${}^3\mathcal{S}_t \cap \partial\mathcal{M}$ embedded in $\partial\mathcal{M}$ with induced metric σ_{ab} .

One starts by deriving the local surface energy-momentum stress tensor

$$\tau^{ab} = \frac{2}{\sqrt{-h}} \frac{\delta I}{\delta h_{ab}}, \quad (35)$$

which characterizes the entire system, including contributions from gravitation and (if present) matter. It is related to the stress energy tensor $T^{ab} = \frac{2}{\sqrt{-g}} \frac{\delta I}{\delta g_{ab}}$ in a rather complicated way.

Then, for any Killing vector field ξ^a associated with an isometry of the boundary three-metric, one defines the conserved charge ⁵

$$Q_\xi = \int_\Sigma d^2x \sqrt{\sigma} u_a \tau^{ab} \xi_b . \quad (36)$$

Now, a straightforward application of (35) with the action (25) gives

$$\tau^{ab} = -\frac{1}{8\pi G} \left[(K^{ab} - h^{ab} K) + \frac{2}{l} h^{ab} - l \left(\mathcal{R}^{ab} - \frac{1}{2} h^{ab} \mathcal{R} \right) \right] . \quad (37)$$

The first term on the right-hand side of Eq. (37) results from the boundary term in the action, while all other terms are due to the presence of the counterterms we added in order to have finite quantities, when the boundary is sent to infinity. Employing the AdS/CFT correspondence, the result (37) can also be interpreted as the expectation value of the stress tensor in the boundary conformal field theory. In the case of the Kerr-Newman-AdS geometry, we choose $\partial\mathcal{M}$ to be a three-surface of fixed r , and obtain for τ^{ab}

$$\begin{aligned} 8\pi G \tau_{tt} &= \frac{2m}{rl} + \mathcal{O}(1/r^2) , \\ 8\pi G \tau_{t\phi} &= -\frac{2ma}{rl\Xi} \sin^2 \theta + \mathcal{O}(1/r^2) , \\ 8\pi G \tau_{\phi\phi} &= \frac{m}{rl\Xi^2} \sin^2 \theta [l^2 + 3a^2 \sin^2 \theta - a^2] + \mathcal{O}(1/r^2) , \\ 8\pi G \tau_{\theta\theta} &= \frac{ml}{r\Delta_\theta} + \mathcal{O}(1/r^2) , \end{aligned} \quad (38)$$

all other components vanishing. As expected, the presence of counterterms cures also the divergences of the charges. In fact we get

$$M = Q_{\partial_t/\Xi} = \frac{m}{\Xi^2} , \quad (39)$$

$$J = Q_{\partial_\phi} = \frac{am}{\Xi^2} , \quad (40)$$

in full agreement with the results (18) obtained with Komar integrals.

⁵Note that in the conventions of [34] an additional minus sign appears in the conserved charges (36); this comes from the fact that the definition of the extrinsic curvatures in [34] differs from ours by a factor of -1 .

IV. THERMODYNAMICS

A. Generalized Smarr Formula

Using the expressions (18) for mass and angular momentum, (9) for the horizon area, and the fact that $\Delta_r = 0$ for $r = r_+$, one obtains by simple algebraic manipulations a generalized Smarr formula for Kerr-Newman-AdS black holes, which reads

$$M^2 = \frac{\mathcal{A}}{16\pi} + \frac{\pi}{\mathcal{A}}(4J^2 + Q^4) + \frac{Q^2}{2} + \frac{J^2}{l^2} + \frac{\mathcal{A}}{8\pi l^2} \left(Q^2 + \frac{\mathcal{A}}{4\pi} + \frac{\mathcal{A}^2}{32\pi^2 l^2} \right). \quad (41)$$

In the limit $l \rightarrow \infty$ this formula reduces to the usual Smarr formula for asymptotically flat Kerr-Newman solutions [35,36], so one can consider the last two terms on the right-hand side as AdS corrections.

Relation (41) holds for classical black holes, and contains as usual all the information about the thermodynamic state of the black hole, taking the black hole entropy to be one quarter of the horizon area⁶,

$$S = \frac{\mathcal{A}}{4}. \quad (42)$$

In the next subsection, we shall check Eq. (42) using the Euclidean actions (33), (34), and standard thermodynamical relations.

We may then regard the parameters S , J and Q as a complete set of energetic extensive parameters for the black hole thermodynamical fundamental relation $M = M(S, J, Q)$,

$$M^2 = \frac{S}{4\pi} + \frac{\pi}{4S}(4J^2 + Q^4) + \frac{Q^2}{2} + \frac{J^2}{l^2} + \frac{S}{2\pi l^2} \left(Q^2 + \frac{S}{\pi} + \frac{S^2}{2\pi^2 l^2} \right). \quad (43)$$

One can then define the quantities conjugate to S , J and Q . These are the temperature

$$T = \left. \frac{\partial M}{\partial S} \right|_{JQ} = \frac{1}{8\pi M} \left[1 - \frac{\pi^2}{S^2} (4J^2 + Q^4) + \frac{2}{l^2} \left(Q^2 + \frac{2S}{\pi} \right) + \frac{3S^2}{\pi^2 l^4} \right], \quad (44)$$

the angular velocity

$$\Omega = \left. \frac{\partial M}{\partial J} \right|_{SQ} = \frac{\pi J}{MS} \left(1 + \frac{S}{\pi l^2} \right), \quad (45)$$

and the electric potential

$$\Phi = \left. \frac{\partial M}{\partial Q} \right|_{SJ} = \frac{\pi Q}{2MS} \left(Q^2 + \frac{S}{\pi} + \frac{S^2}{\pi^2 l^2} \right). \quad (46)$$

These expressions reduce to the corresponding asymptotically flat Kerr-Newman expressions in the $l \rightarrow \infty$ limit [36]. The obtained quantities satisfy the first law of thermodynamics

⁶In the following we set $G = 1$.

$$dM = TdS + \Omega dJ + \Phi dQ. \quad (47)$$

Furthermore, by eliminating M from (44)–(46) using (43), it is possible to obtain three equations of state for the KNAdS black holes.

One easily verifies that the relations (44), (45) and (46) for temperature, angular velocity and electric potential respectively, coincide with equations (10), (17) and (20) found in section II.

Another quantity of interest is the thermal capacity $C_{J,Q}$ at constant angular momentum and charge, which, as we shall see in section IV C, is relevant in the stability analysis of the canonical ensemble. It reads

$$\begin{aligned} C_{J,Q} = T \left. \frac{\partial S}{\partial T} \right|_{JQ} &= \frac{4\pi^{-1} M T S^3}{4J^2 + Q^4 - 4T^2 \frac{S^3}{\pi} + \frac{2S^3}{\pi^3 l^2} + \frac{3S^4}{\pi^4 l^4}} \\ &= \frac{4\pi M T S}{1 - 4\pi T (2M + TS) + \frac{2}{l^2} \left(Q^2 + \frac{3S}{\pi} \right) + \frac{6S^2}{\pi^2 l^4}}. \end{aligned} \quad (48)$$

In the above discussion, we have treated the cosmological constant as a fixed parameter; however, as shown by Henneaux and Teitelboim [37], it is possible to induce it from a three form gauge potential coupled to the gravitational field. The interest of this mechanism resides in that it follows from Kaluza-Klein reduction of supergravity theories [38], and in particular it is relevant for the compactification of M-theory on S^7 . We can thus promote the cosmological constant to a thermodynamic state variable. Its conjugate variable Θ reads

$$\Theta = \left. \frac{\partial M}{\partial \Lambda} \right|_{SJQ} = -\frac{1}{2M} \left[\frac{1}{3} J^2 + \frac{S}{6\pi} \left(Q^2 + \frac{S}{\pi} \right) - \frac{\Lambda S^3}{18\pi^3} \right]. \quad (49)$$

Now we can consider ensembles where Λ is allowed to fluctuate, and the first law reads

$$dM = TdS + \Omega dJ + \Phi dQ + \Theta d\Lambda. \quad (50)$$

Finally, if we regard M as a function of S , J , Q^2 and Λ , it is a homogeneous function of degree $1/2$. Applying Euler's theorem we obtain

$$\begin{aligned} \frac{1}{2} M &= TS + \Omega J + \frac{1}{2} \Phi Q - \Theta \Lambda \\ &= TS + \Omega J + \frac{1}{2} \Phi Q - \frac{S}{2\pi l^2} \left[\frac{\Phi S}{\pi Q} + \frac{\Omega J}{1 + \frac{S}{\pi l^2}} \right]. \end{aligned} \quad (51)$$

Again, sending l to infinity we recover the usual Smarr law, and the last term is an AdS correction.

B. Thermodynamic Potentials from the Euclidean Action

We now turn to the definition of the thermodynamic potentials from the Euclidean actions (34) and (33), relevant for the canonical and the grand-canonical ensemble respectively. Let us first treat the latter case. The Gibbs potential $G(T, \Omega, \Phi)$ is defined by

$$G(T, \Omega, \Phi) = \frac{I}{\beta}, \quad (52)$$

with I given by (33). Using the expressions (10) for the temperature, (17) for the angular velocity, and (20) for the electric potential, we get after some algebra the corresponding extensive quantities

$$S = - \left. \frac{\partial G}{\partial T} \right|_{\Omega\Phi}, \quad J = - \left. \frac{\partial G}{\partial \Omega} \right|_{T\Phi}, \quad Q = - \left. \frac{\partial G}{\partial \Phi} \right|_{T\Omega}, \quad (53)$$

which turn out to coincide precisely with the expressions (42), (18) and (19). One further readily verifies that

$$G(T, \Omega, \Phi) = M - \Omega J - TS - \Phi Q, \quad (54)$$

which means that G is indeed the Legendre transform of the energy $M(S, J, Q)$ (cf. (43)) with respect to S, J and Q .

As for the canonical ensemble, the Helmholtz free energy is defined by

$$F(T, J, Q) = \frac{\tilde{I}}{\beta} + \Omega J, \quad (55)$$

with \tilde{I} given by (34). The term ΩJ comes from the needed Legendre transformation to hold the angular momentum fixed. Using the relations (10) for the temperature, (18) for the angular momentum, and (19) for the electric charge, one verifies that the conjugate quantities

$$S = - \left. \frac{\partial F}{\partial T} \right|_{JQ}, \quad \Omega = \left. \frac{\partial F}{\partial J} \right|_{TQ}, \quad \Phi = \left. \frac{\partial F}{\partial Q} \right|_{TJ}, \quad (56)$$

agree with expressions (42), (17) and (20). Furthermore one easily shows that

$$F(T, J, Q) = M - TS, \quad (57)$$

so F is in fact the Legendre transform of $M(S, J, Q)$ with respect to S .

C. Stability Analysis

The stability of a thermodynamical system with respect to small variations of the thermodynamic coordinates, is usually studied by analyzing the behaviour of the entropy $S(M, J, Q)$. The stability requires that the entropy hypersurface lies everywhere below its family of tangent hyperplanes, as to say that the entropy must be a concave function of the entropic extensive parameters. This will place some restrictions on physical observables. For example, the thermal capacity must be positive in any stable system. The stability can also be studied by using other thermodynamic potentials, as for example the energy or its Legendre transforms, which have to be convex functions of their extensive variables, and concave functions of their intensive variables. The use of one thermodynamic potential with

respect to another is of course a matter of convenience, depending on the ensemble one is dealing with. Here we are mainly interested in finding the zones where the system is locally stable. These are bounded by “critical” hypersurfaces, on which

$$\det \left(\frac{\partial^2 S}{\partial X_i \partial X_j} \right) = 0, \quad (58)$$

where $X_i = M, J, Q$.

In the canonical ensemble, charges and angular momentum are fixed parameters and for this reason, the positivity of the thermal capacity $C_{J,Q}$ is sufficient to assure stability [17]. This means that the points (hypersurfaces) where $C_{J,Q}$ vanishes or diverges represent the critical hypersurfaces we are looking for. The equation of such surfaces can easily be obtained by deriving the expression for T , Eq. (44) (where M is given by (43)), with respect to S and requiring it to vanish (or to diverge). One can see that the equation $\partial T / \partial S = 0, \infty$ has only one physically acceptable solution, which reads ⁷

$$\begin{aligned} J^2 = & - \frac{3S^2(\pi + S)^2(\pi + 2S) + \pi^4 Q^4(3\pi + 2S) + 2\pi^3 Q^2 S(2\pi + 3S)}{4\pi^4(3\pi + 4S)} \\ & + \frac{S}{2\pi^4(3\pi + 4S)} \left[\pi^8 Q^8 + 6\pi^3 Q^2 S(\pi + S)^4 - 2\pi^7 Q^6(2\pi + 3S) \right. \\ & \quad \left. + S^2(\pi + S)^3(3\pi^3 + 10\pi^2 S + 15\pi S^2 + 9S^3) \right. \\ & \quad \left. + \pi^4 Q^4(4\pi^4 + 9\pi^3 S + 6\pi^2 S^2 + 6\pi S^3 + 6S^4) \right]^{\frac{1}{2}}. \end{aligned} \quad (59)$$

In the grand-canonical ensemble the critical surfaces can be determined by requiring that the determinant of the whole Hessian of the Gibbs potential $G(T, \Omega, \Phi)$ be vanishing (diverging) [17]. This yields an equation which can easily be resolved for the charge parameter q . The result is

$$q^2 = - \frac{-a^4 - 2a^2 r_+^2 - 2a^4 r_+^2 - r_+^4 - a^4 r_+^4 + 2r_+^6 + 2a^2 r_+^6 + 3r_+^8}{-3a^2 + r_+^2 + a^2 r_+^2 + r_+^4}. \quad (60)$$

These stability conditions will be analyzed in the following subsections.

D. Canonical Ensemble

In the canonical ensemble, we study the black holes holding the temperature T , the angular momentum J and the charge Q fixed. The associated thermodynamic potential is the Helmholtz free energy $F(T, J, Q)$ (55). We shall analyze the thermodynamics in this ensemble in the (T, J) -plane, keeping the charge fixed. It immediately follows that in this plane the extremal black hole solutions are represented by the ordinate axis $T = 0$, and the half-plane $T > 0$ corresponds to the nonextremal solutions.

⁷In the following we set $l = 1$.

We shall begin by considering the local stability of the black holes. As explained in Section IV C, local stability in the canonical ensemble is equivalent to the positivity of the thermal capacity (48). The behaviour of the thermal capacity can be more easily understood from the state equation $T = T(S, J, Q)$ at fixed J and Q , Eq. 44. In figure 1 we have reported

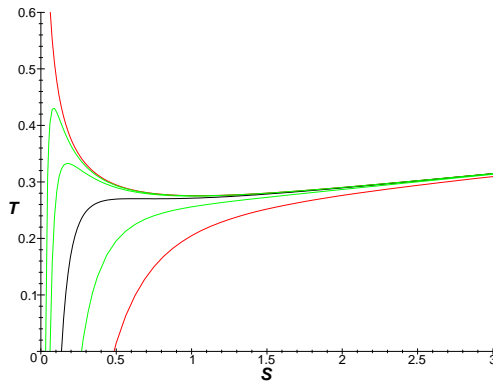


FIG. 1. State equation $T = T(S)$. The plot shows the $T(S)$ curves at fixed $Q = 0$ for $J = 0$ (the upper curve), 0.005, 0.01, 0.0236, 0.05 and 0.1 (the lower curve). For $J_c \approx 0.0236$ the local extrema merge in a point of inflection, and for higher J the curve is monotonically increasing. For $Q \neq 0$, see the text.

these curves for $Q = 0$ and different values of J . When $J = 0$, the usual Schwarzschild-AdS behaviour is reproduced; the curve first decreases towards a minimum, corresponding to the branch of small unstable black holes, then increases along the branch of large stable black holes. As soon as $J \neq 0$, a branch of stable small black holes appears, separated from the branch of large black holes by intermediate unstable black holes. This results in the appearance of two phases in the canonical ensemble, a small black hole phase and a large black hole phase, in analogy to what was found in [10] for charged AdS black holes and in [8] for stringy-corrected black holes. While J grows, the local maximum of $T(S)$ decreases, and eventually degenerates for $J_c \approx 0.0236$ into a point of inflection, signalling a second order phase transition for the Kerr-AdS black hole. For $J > J_c$, the curve $T(S)$ is monotonically increasing, and we are left with a unique phase of black holes. The behaviour near this critical point is completely analogous to a liquid/vapour system described by the Van der Waals equation.

In the Kerr-Newman-AdS case, one can repeat this analysis along the same lines; for $0 < Q < Q_c$, where $Q_c \approx 0.166$, we obtain a behaviour analogous to that of the Kerr-AdS black hole, with the difference that the stable small black hole branch appears already at zero angular momentum [10]. It is then possible to obtain the critical value $J_c(Q)$, where the point of inflection is located, as a function of the charge. For $Q = Q_c$ the small black hole phase disappears, and for larger values of the charge the function $T(S)$ is monotonically increasing for any angular momentum, and hence a unique stable black hole phase exists; the curve of second order critical points ends in $J = 0$, $Q = Q_c$. The resulting phase diagram is shown in figure 2; the solid line corresponds to the second order critical points. Inside the curve we have a region where two phases of black holes are allowed, with a first order

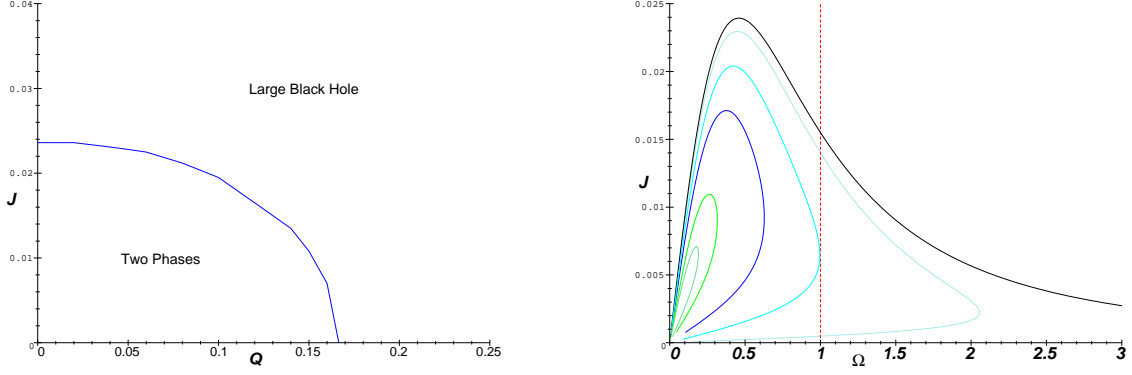


FIG. 2. Phase Diagram in the (Q, J) -plane and stability diagram in the (Ω, J) -plane. In the left plot the curve corresponds to a line of second order critical points. Outside the region bounded by it, there is a unique black hole phase. Inside the region, one has a small black hole phase at low temperatures and a large black hole phase at high temperatures, separated by a first order phase transition. In the right plot we have drawn the lines where the thermal capacity diverges, for $Q = 0, 0.05, 0.091, 0.12, 0.15$ and 0.16 respectively from the outer to the inner curve. Outside these regions the thermal capacity is positive. The vertical line represents the limit where $\Omega = 1/l$; for $Q > 0.091$ the entire instability region has $\Omega < 1/l$.

transition between a small black hole phase and a large black hole phase as the temperature is increased, the two phases being separated by a coexistence curve.

In the second graph of figure 2 we have visualized the instability region in the (Ω, J) -plane. In the uncharged case we have stable black holes for large J and thermodynamic instability below the curve. As Q grows, the instability region shrinks and disappears for the critical charge Q_c . The points inside the instability region correspond to mixed phases of small/large black holes, obtained by means of a Maxwell-like construction.

The phase diagrams in the (T, J) -plane for the canonical ensemble are shown in figure 3. The left diagram corresponds to the uncharged Kerr-AdS black hole, while the one on the right side is plotted for $Q = 0.05$ and shows the qualitative behaviour of the Kerr-Newman-AdS black holes with electric charge ranging in the interval $0 < Q < Q_c$. In these diagrams, we have plotted the curves on which the specific heat diverges. Outside the region bounded by them, every point (T, J, Q) of the diagram corresponds to a single black hole solution, which is locally stable (its thermal capacity is positive). In contrast, inside the regions bounded by these curves, which are indicated by $C < 0$ in the figure, every point (T, J, Q) corresponds in fact to three different black hole solutions. To elucidate this point let us go back to the curves $T(S)$ of figure 1. The divergence of the thermal capacity obviously corresponds to the local extrema of $T(S)$. For every temperature between that of the local minimum and that of the local maximum of $T(S)$, we have three black holes: a small metastable black hole, an unstable intermediate one, and a large stable one, which are represented by a single point in the (T, J, Q) -diagram. If we start from a small stable black hole and increase its temperature while holding J and Q fixed, as we reach the temperature of the local minimum of $T(S)$, it undergoes a first order phase transition with a jump in the

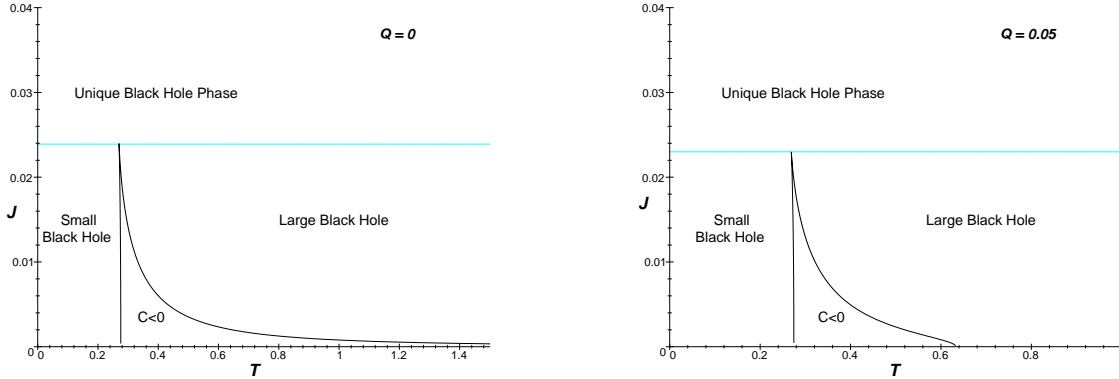


FIG. 3. Phase diagrams in the (T, J) - plane. The phase diagram of the $Q = 0$ Kerr-AdS black hole is plotted on the left, while the diagram for Kerr-Newman-AdS black holes with charge $0 < Q < Q_c \approx 0.166$ is shown on the right. For higher charge the diagram is trivial, as one is left with a unique stable black hole phase. The left branch of the solid curve is the first order small/large phase transition curve. It ends in a cusp, where a second order phase transition occurs.

entropy, and reaches the black hole represented by the local minimum of $T(S)$. Then, the state will follow the branch of large stable black holes. Hence the low temperature branch of the $C_{JQ} = \infty$ curve corresponds to a first order phase transition line between a small black hole phase and a large black hole phase. This line ends in a critical point located in the cusp, where the transition degenerates to a second order phase transition. Then, inside the region bounded by the $C_{JQ} = \infty$ curve, the thermodynamically stable state is simply a locally stable large black hole phase. Finally, for Kerr-Newman-AdS black holes with charge $Q > Q_c$ the instability region and the small/large transition disappear, leaving a unique phase of stable black holes.

The local stability is however not sufficient to ensure global stability; the full problem is very hard to tackle, but we could at least try to compare the free energy of the black hole with that of some reference background like thermal AdS space, which can lead to a Hawking-Page phase transition [5]. In doing so, however, one encounters the problem that pure AdS space is not a solution of the Einstein-Maxwell equations with fixed electric charge Q as boundary condition. Furthermore, AdS space has no angular momentum, as $J = 0$ for $m = 0$ (cf. (18)). Therefore, it is not a suitable reference background in the canonical ensemble, which has fixed Q and J . One should compare the free energy of the black hole with that of other possible solutions, such as AdS space filled with a gas of charged particles carrying also angular momentum J , or a Kerr-Newman-AdS black hole with part of the total charge and angular momentum carried by a gas of such particles gravitating outside its horizon [11]. Only for $Q = J = 0$, i. e. the Schwarzschild-AdS black hole, pure AdS space contributes to the path integral and should be taken into account, as it was done in [5]. In the charged rotating case, however, the question of global stability and Hawking-Page phase transitions remains unsettled.

Finally, we have to examine the stationarity condition $\Omega < 1/l$, which is needed to have thermodynamic equilibrium, and a well-defined holographic thermal state in the boundary

CFT. The curve $\Omega = 1/l$ can be defined parametrically in the (T, J) -plane by the equations

$$\begin{aligned} J^2 &= \frac{S}{4\pi^4(S + \pi)} (S^2 + \pi S + \pi^2 Q^2)^2, \\ T^2 &= \frac{1}{16} \frac{(2S + \pi)^2 (S^2 + \pi S - \pi^2 Q^2)^2}{\pi^2 S^3 (S + \pi)^3}, \end{aligned} \quad (61)$$

with

$$S \in \left[\frac{\pi}{2} \left(\sqrt{1 + 4Q^2} - 1 \right), +\infty \right]. \quad (62)$$

The lower bound corresponds to supersymmetric black holes for $Q \neq 0$, and for $S \rightarrow \infty$ the curve is always asymptotic to $T = 1/(2\pi l)$. The behaviour of the curve depends on

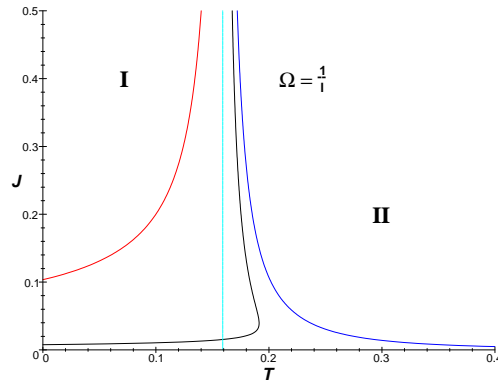


FIG. 4. $\Omega = 1/l$ curves. These curves have been plotted for the values $Q = 0$, $Q = 0.2$ and $Q = 0.5$ of the charge, from the right to the left respectively. The vertical line is the asymptote $T = 1/(2\pi l)$. For charges $0 < Q < 1/\sqrt{8}$ the qualitative behaviour is similar to the intermediate curve, while for higher charges the corresponding curves behave like the one with $Q = 0.5$. In region *I* we have $\Omega > 1/l$ and in region *II* we have $\Omega < 1/l$. The intersection of these curves with the $T = 0$ axis corresponds to supersymmetric black holes.

the electric charge, and has been summarized in figure 4. For $Q = 0$, the curve is strictly decreasing from the asymptote and ends at $J = 0$ for infinite temperature. If $0 < Q < 1/\sqrt{8}$, the infinite temperature branch is deformed, curves back towards the J axis and intersects it in the supersymmetric point. Finally, for $Q > 1/\sqrt{8}$, the curve remains at $T < 1/2\pi l$, and is strictly increasing from its intersection with the ordinate axis, again describing a supersymmetric black hole, to the asymptote. In any case the $\Omega = 1/l$ curve splits the (T, J) -plane into two regions, named *I* and *II* in figure 4. Black holes in region *I*, at the left of the $\Omega = 1/l$ curve, spin at angular velocity Ω greater than $1/l$ and show superradiant instability. On the other hand, black holes in region *II*, at the right of the curve, have $\Omega < 1/l$, and have a well-defined thermodynamics. However, this is not the whole story. Inside the regions of local instability shown in figure 3, every point (T, J, Q) corresponds in fact to three black hole solutions: an unstable, a metastable and a locally stable black hole.

It is possible to verify that the locally stable one spins at $\Omega < 1/l$, and hence the whole region of $\Omega < 1/l$ black holes is the union of region *II* and the instability region. This stems from the fact that the locally stable black hole, at fixed (T, J, Q) , is the one with maximum entropy, and that $\Omega(S, J, Q)$ is a decreasing function of S at fixed J and Q .

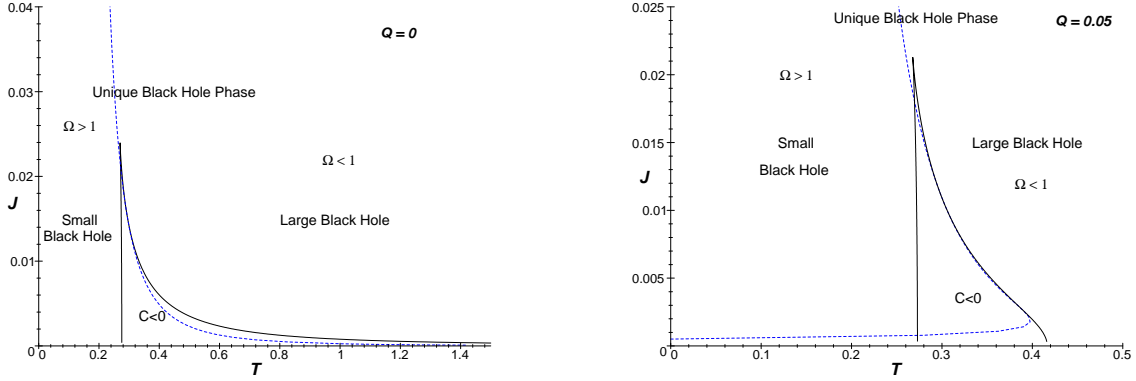


FIG. 5. Phase diagrams with $\Omega = 1/l$ curve, for charges $Q = 0$ and $Q = 0.05$. The second diagram is characteristic for all black holes with $0 < Q < Q_c$. The dotted curve represents the line $\Omega = 1/l$.

The full phase diagram, taking into account the restriction on the angular velocity, is reported in figure 5. It implies that part of the small/large black hole phase transition has no dual CFT analogue, as in this region one has $\Omega > 1/l$, and so the Einstein universe in which the dual CFT lives would have to rotate faster than light. However the second order critical point lies in the $\Omega < 1/l$ region. Furthermore, for charged black holes, the first order phase transition occurs at $\Omega < 1/l$ for sufficiently small angular momentum, and has therefore an analogue on the CFT side.

E. Grand-Canonical Ensemble

As described in Section IV B, the thermodynamics of the grand-canonical ensemble can be extracted from the Gibbs potential $G(T, \Omega, \Phi)$. The natural variables for this ensemble are the intensive parameters T, Ω and Φ ; however, to simplify the analysis, we shall study the thermodynamics in the (r_+, a) -plane, at fixed electric potential Φ .

In this plane, the black holes with genuine event horizon are restricted to the region $a_{\text{extr}}^-(r_+, \Phi) \leq a \leq a_{\text{extr}}^+(r_+, \Phi)$ with $a < l$, where

$$a_{\text{extr}}^{\pm}(r_+, \Phi) = \frac{r_+}{2l^2|\Phi|} \left(r_+^2 - l^2 + 2l^2\Phi^2 \pm \sqrt{(r_+^2 - l^2)^2 + 16r_+^2 l^2 \Phi^2} \right)^{1/2}. \quad (63)$$

Between these two curves the black holes have a bifurcate horizon, on the curves they are extremal, and outside the solution shows a naked singularity. If $|\Phi| \leq 1$, a_{extr}^- is negative, and the entire region below the curve $a_{\text{extr}}^+(r_+, \Phi)$ represents black hole solutions. For $\Phi > 1$,

a_{extr}^- is positive for $0 \leq r_+ \leq l\sqrt{(\Phi^2 - 1)/3}$; if r_+ lies in this range, a_{extr}^- determines a new region with naked singularities, and the black holes are found between the two curves. For r_+ outside of this interval, all the points represent black holes, as long as $a < l$. Finally, in the limit $\Phi \rightarrow \infty$, the two curves merge and only a line of extremal black holes with $r_+ = a < l$ survives.

Another relevant information in the thermodynamic diagram is given by the region where the Killing vector $\partial_t + \Omega_H \partial_\phi$ is timelike all the way out to infinity. It is easy to see that this condition is satisfied for $a \leq r_+^2/l$, and so is always fulfilled for $r_+ > l$, as we assumed $a < l$. One readily verifies that the condition $a \leq r_+^2/l$ is equivalent to $\Omega < 1/l$. In the diagrams, the region at the right of the curve $a = r_+^2/l$ is the region where the black hole can be in thermal and dynamical equilibrium with radiation, and the rotating Einstein universe at the boundary spins slower than light.

Let us now turn to the stability analysis of the black hole. We shall begin with local stability. The curve separating stable from unstable regions is given by Eq. (60). In fact this equation can be solved for $a(r_+, \Phi)$ after having substituted q in terms of Φ by means of (20); the result is quite complicated, but nevertheless adequate for visualizing the local stability regions in the (r_+, Φ) -plane.

However locally stable black holes can decay into other states with lower free energy. In the case of the grand-canonical ensemble, another possible state is given by AdS space, which can have arbitrary electric potential Φ , constant all over the spacetime. The Gibbs free energy of AdS space filled with thermal radiation vanishes identically, hence the global stability can be investigated by studying the sign of $G(T, \Omega, \Phi)$. The free energy of the black hole is negative for

$$r_+^2(a, \Phi) \geq \frac{l^2}{2} \left(1 - \Phi^2 + \sqrt{(1 - \Phi^2)^2 + \frac{4a^2}{l^2} \Phi^2} \right) \equiv r_{\text{HP}}^2(a, \Phi), \quad (64)$$

which means that the black hole dominates in this region. For $r_+ = r_{\text{HP}}(a, \Phi)$ there is a first order phase transition line, with a discontinuity in the entropy, and for $r_+ < r_{\text{HP}}(a, \Phi)$ the AdS solution is globally preferred. However we stress that this does not exhaust the question of global stability for these black holes, as other solutions with lower free energy may exist [11]. Indeed, there are regions in the (r_+, a) -plane in which the black hole, though being unstable, has lower free energy than AdS space; it is plausible that a new solution exists which minimizes the Gibbs potential.

Finally we observe that the $\Omega = 1/l$ curve, the local stability curve and the Hawking-Page transition curve intersect at the point $(r_+ = l, a = l)$ for any choice of the electric potential. For $\Phi = \Phi_c = 1$ these three curves coincide; for $\Phi < \Phi_c$ we find the $\Omega = 1/l$ curve, the local stability curve and the Hawking-Page transition curve in this order from the left to the right, while for $\Phi > \Phi_c$ they appear in the reverse order.

We have summarized this analysis in figure 6, which shows the phase structure in the (r_+, a) -plane for various values of the electric potential. We see that for $\Phi < \Phi_c = 1$, the Hawking-Page transition curve is the rightmost one; it separates a large r_+ phase of large black holes and an AdS phase, which dominates over black holes with small r_+ . Inside the AdS phase region, with increasing r_+ , we first have a zone of naked singularities separated by the extremality line from a region with genuine black holes, which however do not possess a

boundary CFT analogue, as they have $\Omega > 1/l$, and which are furthermore locally unstable. In the next region we find locally unstable black holes which rotate slower than light, and finally a region with locally stable but globally unstable black holes which ends on the Hawking-Page transition curve. These regions are anyway dominated by the AdS phase. For $\Phi > \Phi_c$ the situation is more subtle; a new branch of extremal black holes appears and bounds a region of naked singularities for small a . For small r_+ we again have the AdS dominated phase, but at the right of the Hawking-Page transition curve we find (a) a region with locally unstable black holes with $\Omega > 1/l$, having however negative Gibbs free energy, so they are preferred with respect to AdS space, (b) a region with stable black holes with $\Omega > 1/l$, and finally (c) a region of stable black holes with $\Omega < 1/l$. This raises the question for region (a) whether there exists at all a thermodynamically stable state for this range of parameters. Furthermore, the region defined by $a < a_{\text{extr}}^-(r_+, \Phi)$ represents naked singularities which have a lower Gibbs free energy than AdS space itself.

V. CONCLUDING REMARKS

In the present paper, we studied the thermodynamics of the four-dimensional Kerr-Newman-AdS black hole both in the canonical and the grand-canonical ensemble. Thereby we encountered an interesting phase structure. In the canonical ensemble, we found a small-large black hole first order phase transition, which disappears for sufficiently large electric charge or angular momentum. In the points where the small-large transition disappears, the first order phase transition degenerates to a higher order one. As pure AdS space is not a solution of the Einstein-Maxwell field equations with fixed electric charge, we cannot compare the black hole Helmholtz free energy with that of pure AdS space, in order to study global stability. It would therefore be desirable to have another reference background to our disposal, which describes AdS space filled with charged rotating particles. Another possibility would be to have a KNAdS black hole surrounded by a gas of particles carrying part of the total charge and angular momentum (cf. the discussion in [11]).

As AdS space can have arbitrary constant electric potential, we can compare the Gibbs free energy of the black hole with that of AdS space in the grand-canonical ensemble. In this way, we found the Hawking-Page transition curve. Also in this context, some intriguing features arise, e. g. one finds black holes which are locally unstable, but nevertheless have lower Gibbs free energy than AdS space itself. There is also a region of naked singularities in the (r_+, a) -phase diagram, which are energetically preferred with respect to AdS space. It would be interesting to study if these naked singularities play some role in the dual CFT.

We hope to have clarified that a consistent treatment of rotating AdS black hole thermodynamics requires the usage of the angular velocity Ω of the rotating Einstein universe, in which the dual conformal field theory lives. This angular velocity differs from that of the event horizon, which enters the thermodynamical description of asymptotically flat black holes. The reason for this discrepancy is that the angular velocity (15) appearing in the canonical form of the metric, does not vanish at infinity. (It even has the opposite sign of Ω_H , cf. (15)). The fact that a consistent thermodynamics can be formulated using Ω is in full agreement with the AdS/CFT correspondence.

The black holes we have considered can also be lifted to eleven dimensions, as solutions of

$\mathcal{N} = 1$, $D = 11$ supergravity [10,39]. These solutions represent the near-horizon limit of M2-branes with spherical worldvolumes, rotating both about an axis of the worldvolume and in planes orthogonal to the worldvolume, the latter rotation giving rise to four R-charges upon Kaluza-Klein compactification. The Kerr-Newman black holes considered here correspond to the special case where all transverse angular momenta of the M2-brane, and hence all R-charges of the black hole, are equal ⁸.

The thermodynamic structure we have elaborated, corresponds then to that of the world-volume field theory of N coincident such branes.

It would be very interesting to give a microscopic description of the Kerr-Newman-AdS black holes in terms of this dual CFT. Let us recall in this context that only black holes whose angular velocity satisfies

$$\Omega \leq \frac{1}{l} \quad (65)$$

correspond to thermal states in the dual field theory, as otherwise the rotating Einstein universe, in which the dual CFT lives, would rotate faster than light. One easily shows that for zero temperature black holes, condition (65) implies

$$q^2 \geq a(a+1)^2 \quad (66)$$

for the electric charge and rotation parameter appearing in the metric. If the bound (66) is saturated, we have a BPS state. It would be interesting to study if the corresponding field theory at weak coupling reproduces the Bekenstein-Hawking entropy of the black hole in this BPS limit. As the M2-brane worldvolume field theory is the strong coupling limit (conformal point) of the D2-brane worldvolume theory [1], the relevant gauge theory would be that on the worldvolume of D2-branes. In any case, in the presence of a global background $U(1)$ current (corresponding to the black hole charge Q), the zero temperature state of the dual field theory must be highly degenerate, as the extremal black hole has nonvanishing entropy⁹. It would also be interesting to consider the five-dimensional case, corresponding to $\mathcal{N} = 4$, $D = 4$ SYM on a rotating Einstein universe [18]. However, the generalization of the rotating five-dimensional AdS black holes found in [18] to nonzero charge seems to be a nontrivial task. If such a solution were known, one could study if there exist BPS states (which can only occur for nonzero charge [18]), and compare their entropy with the one obtained on the CFT side. Apart from the possibility of identifying black hole microstates, this would also be a check of the AdS/CFT correspondence.

⁸A thermodynamical discussion of branes rotating in planes orthogonal to the worldvolume can be found in [40–43,19]. In [40], a field theory model of rotating D3-branes was proposed. This was later generalized in [44] to rotating M-branes.

⁹Note that for zero $U(1)$ current, the extremal black holes have $\Omega > 1/l$ [18], and therefore do not correspond to states in the CFT.

ACKNOWLEDGEMENTS

D. K. has been partially supported by a research grant within the scope of the *Common Special Academic Program III* of the Federal Republic of Germany and its Federal States, mediated by the DAAD.

The authors would like to thank M. M. Taylor-Robinson and L. Vanzo for helpful discussions.

REFERENCES

- [1] J. Maldacena, “The large N limit of superconformal field theories and supergravity,” *Adv. Theor. Math. Phys.* **2** (1998) 231, [hep-th/9711200](#).
- [2] E. Witten, “Anti-de Sitter space and holography,” *Adv. Theor. Math. Phys.* **2** (1998) 253, [hep-th/9802150](#).
- [3] S. S. Gubser, I. R. Klebanov, and A. M. Polyakov, “Gauge theory correlators from noncritical string theory,” *Phys. Lett.* **B428** (1998) 105, [hep-th/9802109](#).
- [4] O. Aharony, S. S. Gubser, J. Maldacena, H. Ooguri, and Y. Oz, “Large N field theories, string theory and gravity,” [hep-th/9905111](#).
- [5] S. W. Hawking and D. N. Page, “Thermodynamics of black holes in anti-de Sitter space,” *Commun. Math. Phys.* **87** (1983) 577.
- [6] E. Witten, “Anti-de Sitter space, thermal phase transition, and confinement in gauge theories,” *Adv. Theor. Math. Phys.* **2** (1998) 505, [hep-th/9803131](#).
- [7] D. Birmingham, “Topological black holes in anti-de Sitter space,” *Class. Quant. Grav.* **16** (1999) 1197, [hep-th/9808032](#).
- [8] M. M. Caldarelli and D. Klemm, “M theory and stringy corrections to anti-de Sitter black holes and conformal field theories,” *Nucl. Phys.* **B555** (1999) 157, [hep-th/9903078](#).
- [9] R. Emparan, “AdS/CFT duals of topological black holes and the entropy of zero energy states,” *JHEP* **06** (1999) 036, [hep-th/9906040](#).
- [10] A. Chamblin, R. Emparan, C. V. Johnson, and R. C. Myers, “Charged AdS black holes and catastrophic holography,” *Phys. Rev.* **D60** (1999) 064018, [hep-th/9902170](#).
- [11] A. Chamblin, R. Emparan, C. V. Johnson, and R. C. Myers, “Holography, thermodynamics and fluctuations of charged AdS black holes,” *Phys. Rev.* **D60** (1999) 104026, [hep-th/9904197](#).
- [12] J. Louko and S. N. Winters-Hilt, “Hamiltonian thermodynamics of the Reissner-Nordström anti-de Sitter black hole,” *Phys. Rev.* **D54** (1996) 2647–2663, [gr-qc/9602003](#).
- [13] C. S. Peça and P. S. José Lemos, “Thermodynamics of Reissner-Nordström anti-de Sitter black holes in the grand canonical ensemble,” *Phys. Rev.* **D59** (1999) 124007, [gr-qc/9805004](#).
- [14] P. Mitra, “Entropy of extremal black holes in asymptotically anti-de Sitter space-time,” *Phys. Lett.* **B441** (1998) 89, [hep-th/9807094](#).
- [15] P. Mitra, “Thermodynamics of charged anti-de Sitter black holes in canonical ensemble,” *Phys. Lett.* **B459** (1999) 119, [gr-qc/9903078](#).
- [16] J. Polchinski, L. Susskind, and N. Toumbas, “Negative energy, superluminosity and holography,” *Phys. Rev.* **D60** (1999) 084006, [hep-th/9903228](#).
- [17] M. Cvetič and S. S. Gubser, “Phases of R charged black holes, spinning branes and strongly coupled gauge theories,” *JHEP* **04** (1999) 024, [hep-th/9902195](#).
- [18] S. W. Hawking, C. J. Hunter, and M. M. Taylor-Robinson, “Rotation and the AdS/CFT correspondence,” *Phys. Rev.* **D59** (1999) 064005, [hep-th/9811056](#).
- [19] S. W. Hawking, “Stability in AdS and phase transitions,” *Talk given at Strings 99, Potsdam (Germany), july 19-24, 1999*.
- [20] R. B. Mann, “Entropy of rotating misner string space-times,” [hep-th/9904148](#).

- [21] D. S. Berman and M. K. Parikh, “Holography and rotating AdS black holes,” *Phys. Lett.* **B463** (1999) 168–173, [hep-th/9907003](#).
- [22] P. C. W. Davies, “Thermodynamic phase transitions of Kerr-Newman black holes in de Sitter space,” *Class. Quant. Grav.* **6** (1989) 1909.
- [23] V. Balasubramanian and P. Kraus, “A stress tensor for anti-de Sitter gravity,” [hep-th/9902121](#).
- [24] R. Emparan, C. V. Johnson, and R. C. Myers, “Surface terms as counterterms in the AdS/CFT correspondence,” *Phys. Rev.* **D60** (1999) 104001 [hep-th/9903238](#).
- [25] P. Kraus, F. Larsen, and R. Siebelink, “The gravitational action in asymptotically AdS and flat space-times,” [hep-th/9906127](#).
- [26] R. B. Mann, “Misner string entropy,” *Phys. Rev.* **D60** (1999) 104047, [hep-th/9903229](#).
- [27] B. Carter, “Hamilton-Jacobi and Schrödinger separable solutions of Einstein’s equations,” *Commun. Math. Phys.* **10** (1968) 280.
- [28] J. F. Plebanski and M. Demianski, “Rotating, charged, and uniformly accelerating mass in general relativity,” *Ann. Phys.* **98** (1976) 98–127.
- [29] V. A. Kosteletsky and M. J. Perry, “Solitonic black holes in gauged N=2 supergravity,” *Phys. Lett.* **B371** (1996) 191–198, [hep-th/9512222](#).
- [30] M. M. Caldarelli and D. Klemm, “Supersymmetry of anti-de Sitter black holes,” *Nucl. Phys.* **B545** (1999) 434, [hep-th/9808097](#).
- [31] G.W. Gibbons and S.W. Hawking, “Action Integrals And Partition Functions In Quantum Gravity,” *Phys. Rev.* **D15** (1977) 2752.
- [32] L. Vanzo, “Black holes with unusual topology,” *Phys. Rev.* **D56** (1997) 6475–6483, [gr-qc/9705004](#).
- [33] S.W. Hawking and S.F. Ross, “Duality between electric and magnetic black holes,” *Phys. Rev.* **D52** (1995) 5865–5876, [hep-th/9504019](#).
- [34] J. D. Brown and J. James W. York, “Quasilocal energy and conserved charges derived from the gravitational action,” *Phys. Rev.* **D47** (1993) 1407–1419.
- [35] L. Smarr, “Mass formula for Kerr black holes,” *Phys. Rev. Lett.* **30** (1973) 71.
- [36] P. C. W. Davies, “The thermodynamic theory of black holes,” *Proc. Roy. Soc. Lond.* **A353** (1977) 499–521.
- [37] M. Henneaux and C. Teitelboim, “Asymptotically anti-de Sitter spaces,” *Commun. Math. Phys.* **98** (1985) 391.
- [38] M. J. Duff, B. E. W. Nilsson, and C. N. Pope, “Kaluza-Klein supergravity,” *Phys. Rept.* **130** (1986) 1.
- [39] M. Cvetič *et. al.*, “Embedding AdS black holes in ten-dimensions and eleven-dimensions,” [hep-th/9903214](#).
- [40] S. S. Gubser, “Thermodynamics of spinning D3-branes,” *Nucl. Phys.* **B551** (1999) 667, [hep-th/9810225](#).
- [41] P. Kraus, F. Larsen and S.P. Trivedi, “The Coulomb branch of gauge theory from rotating branes,” *JHEP* **03** (1999) 003, [hep-th/9811120](#).
- [42] R. G. Cai and K. S. Soh, “Critical behavior in the rotating D-branes,” *Mod. Phys. Lett.* **A14** (1999) 1895, [hep-th/9812121](#).
- [43] R. G. Cai and K. S. Soh, “Localization instability in the rotating D-branes,” *JHEP* **05** (1999) 025, [hep-th/9903023](#).

- [44] M. Cvetič and S. S. Gubser, “Thermodynamic stability and phases of general spinning branes,” *JHEP* **07** (1999) 010, [hep-th/9903132](#).

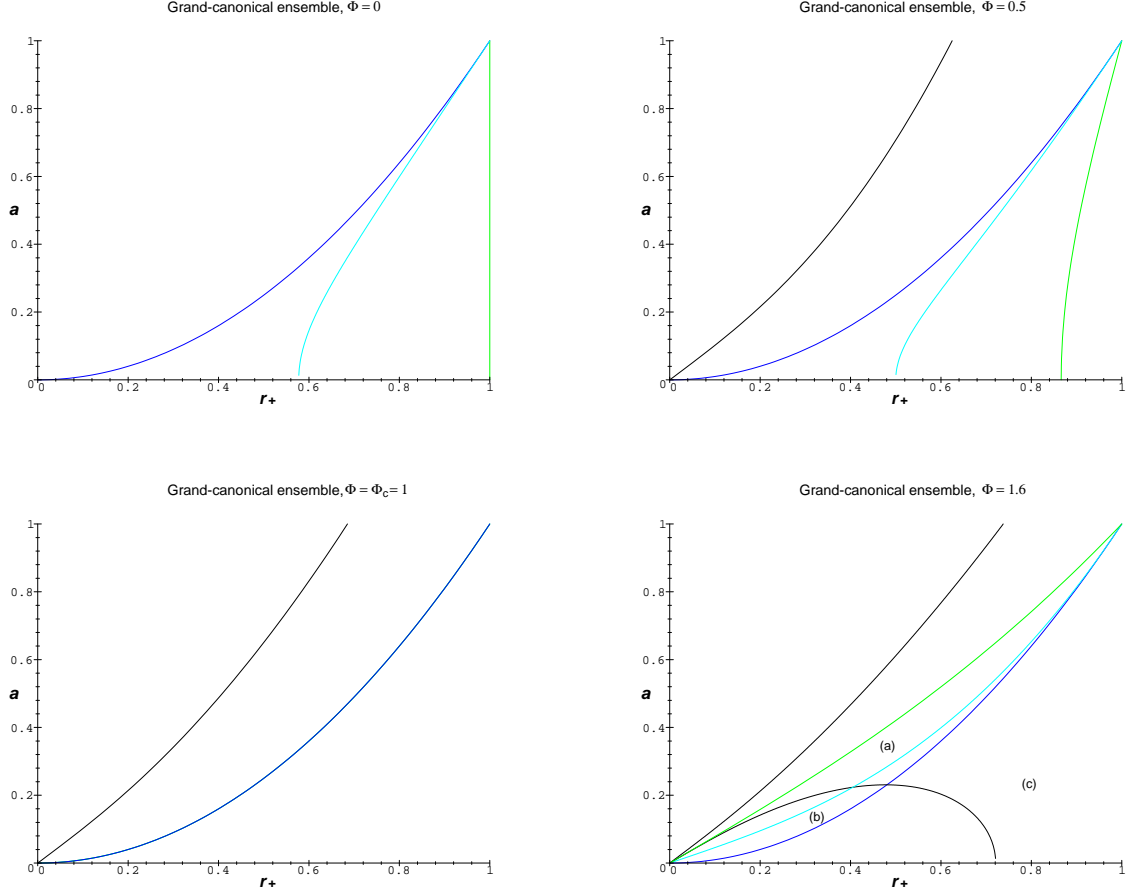


FIG. 6. Phase structure in the grand-canonical ensemble in the (r_+, a) -plane, for various values of the electric potential Φ . For $\Phi = 0$ we have, from the left to the right, the $\Omega = 1/l$ curve, the line bounding the stability region, and the Hawking-Page transition curve. For $0 < \Phi < \Phi_c = 1$, in addition to these three lines, the extremality curve appears at the left. For the critical potential $\Phi = \Phi_c$, the $\Omega = 1/l$ curve, the stability bound, and the Hawking-Page transition line coalesce. Finally, for $\Phi > \Phi_c$, an additional extremality line appears (the one intersecting the r_+ axis twice), and the order of the $\Omega = 1/l$ curve, the stability bound, and the Hawking-Page transition line is reversed. The various regions bounded by these curves are discussed in the text.